Journal of Electroceramics 5:1, 21–30, 2000

Defect Chemistry of $SrBi_2Ta_2O_9$ and Ferroelectric Fatigue Endurance

A.C. PALANDUZ* & D.M. SMYTH
Materials Research Center, Lehigh University, 5 E. Packer Ave., Bethlehem, PA 18015, USA

Submitted July 9, 1999; Revised December 3, 1999; Accepted December 14, 1999

Abstract. The defect chemistry and charge transport properties of doped and undoped $SrBi_2Ta_2O_9$ (SBT) were studied by making 4-point dc equilibrium electrical conductivity, thermopower, ionic transport number, X-ray diffraction (XRD), and X-ray photoelectron spectroscopy (XPS) measurements. Results of high temperature equilibrium dc conductivity, thermoelectric power, and transport number measurements as a function of oxygen activity in the temperature range 650–725°C revealed that undoped SBT displays a broad centrally located plateau of ionic conductivity with an activation energy of mobility of 0.94 eV and a prominent upturn at high oxygen activity, caused by p-type conductivity. The effects of acceptor and donor dopants are consistent with a 1–2% net acceptor excess in the undoped compound. It has been observed that there is substantial (several percent) cation place exchange between the Sr^{2+} and Bi^{3+} in SBT. It is proposed that the net acceptor excess in undoped SBT consists of disordered Sr^{2+} substituting for Bi^{3+} in the fluorite-like bismuth oxide layers which are locally compensated by oxygen vacancies. The formation of the net donor excess by disordered Bi^{3+} substituting for Sr^{2+} in the perovskite-like layers does not manifest itself as n-type conductivity behavior, because the band gap is large and the mobility is highly thermally activated. The superior intrinsic ferroelectric fatigue endurance of SBT is attributed to the lack of mobile charged defects in the perovkite-like layers which create the ferroelectric response of the compound. The metallic bismuth presence on the surface of undoped SBT, as revealed by qualitative XPS measurements, is believed to result from long exposure to the highly reducing conditions in the XPS system.

Keywords: SBT, ferroelectric fatigue endurance, defect chemistry, cation place exchange, local charge compensation

1. Introduction

Nonvolatile thin film memory applications of $SrBi_2Ta_2O_9$ (SBT) are of increasing interest to the scientific community [1]. The detrimental influence of oxygen vacancies and electronic defects on the ferroelectric properties of perovskite compounds are known [2–5]. The defect chemistry and charge transport properties of SBT, which has a superior intrinsic ferroelectric fatigue endurance, are of interest, for they may bring new insight into the relationship between defect chemistry and ferroelectric fatigue, and lead to the discovery of new phenomena in the layered bismuth oxides.

*Crystal Physics and Electroceramics Laboratory, Department of Materials Science and Engineering, Massachusetts Institute of Technology, Cambridge, MA 02139, USA.

2. Experimental

SBT samples were prepared by the mixed oxide technique, using a modified version of Subbarao's recipe [6]. The starting powders used for processing the ceramic samples are given in Table 1.

The ball-milled mixture of starting powders were calcined in a Pt crucible at 1100°C for 1 h in air in order to form SBT. Hydrostatically pressed samples were sintered at 1200°C for 30 min in a double

Table 1. The purity and supplier of each starting powder used in the synthesis of undoped and doped SBT

Compound	Supplier	Purity
$SrCO_3$	Johnson Matthey Company, Inc.	99.99%
Bi_2O_3	Johnson Matthey Company, Inc.	99.9998% Puratronic
Bi_2O_3	Morton Thiokol, Inc.	Ultrapure
Ta_2O_5	Johnson Matthey Company, Inc.	99.993% Puratronic
Ta_2O_5	Johnson Matthey Company, Inc.	99.9%
La_2O_3	Johnson Matthey Company, Inc.	99.99%
TiO_2	Johnson Matthey Company, Inc.	99.995% Puratronic

crucible arrangement, embedded in calcined SBT packing powder.

XRD measurements were made with a Philips APD 1700 automated powder diffractometer system using Cu $\alpha 1$ radiation.

High temperature equilibrium electrical conductivity measurements were made by the standard 4-point dc technique using Pt electrodes in a flowing gas stream composed of Ar-O_2 mixtures or CO_2 depleted of O_2 by means of an electrochemical oxygen pump using CaO-doped ZrO_2. In order to minimize Bi_2O_3 loss during the conductivity measurements, a small amount of undoped SBT powder, which presumably would provide a protective Bi_2O_3 atmosphere, was placed under an alumina cover near the sample. The oxygen activity near the sample was measured with a yttria-doped zirconia electrochemical sensor. The electrical noise level in the samples was very high all through the $P_{(O_2)}$ range in which conductivity measurements were made.

Thermoelectric power measurements were made using a heat pulse technique, similiar to that developed by [7]. A sintered undoped SBT sample was equilibriated at 650°C in a flowing O_2 stream. One end of the sample was heated by passing an ac current through a heater Pt wire for less than two minutes, creating a temperature difference of about 35°C across the two ends of the sample. Such a large temperature difference was created across the sample so that clear readings could be obtained during the cooling stage of the experiment despite the very high electrical noise level that existed in SBT. The thermoelectric voltage developed and the voltage signal proportional to the temperature difference across the sample were measured as a function of time, as the temperature gradient decreased.

Oxygen concentration cells were used in order to measure the ionic transport number t_i of sintered undoped SBT discs. Sintered yttria-doped zirconia discs were used as the reference electrolyte. Pt nets, with a Pt lead wire tied to each, were attached to the opposing faces of SBT and yttria-doped zirconia discs. The faces were then lightly painted with Pt paste in order to form porous electrodes. The same oxygen activity $P_{(O_2)}$ interval was applied across the thickness of both SBT and reference discs for each t_i measurement. Softened glass seals were used to prevent the gas on one side of the discs from leaking to the other side at the elevated temperature of 645°C at which the experiment was run. The four different oxygen activity intervals in which the measurements were made are given in Table 2.

Table 2. Oxygen activity intervals used in making the ionic transport number measurements

Data No.	Side A (atm.)	Side B (atm.)	$\log P_{avg(O_2)}$ (atm.)
1	Air	O_2	
	$\log P^A_{(O_2)} = -0.68$	$\log P^B_{(O_2)} = 0.02$	-0.20
2	Air	Ar-O_2 mixture	
	$\log P^A_{(O_2)} = -0.68$	$\log P^B_{(O_2)} = -1.84$	-0.95
3	Ar-O_2 mixture	Ar	
	$\log P^A_{(O_2)} \approx -1.84$	$\log P^B_{(O_2)} = -4.03$	-2.14
4	Ar	Ar	
	$\log P^A_{(O_2)} \approx -4$	$\log P^B_{(O_2)} = -4.02$	-4.01

Log $P_{avg(O_2)}$ is defined as log $P_{avg(O_2)} \equiv \log[(P^A_{(O_2)} + P^B_{(O_2)})/2]$, where $P^A_{(O_2)}$ and $P^B_{(O_2)}$ are the oxygen partial pressures on the two faces A and B of the discs, respectively. When the same oxygen activity interval is imposed on both of the SBT and reference discs, the approximate ionic transport number t_i for undoped SBT can be obtained by taking the ratio of emfs generated across SBT and the reference electrolyte.

XPS measurements have been performed with a Scienta ESCA-300 system using Al Kα radiation in order to monitor the state of bismuth both on the surface and on a freshly-formed fracture surface created in the ultra-high vacuum chamber to represent the interior of SBT.

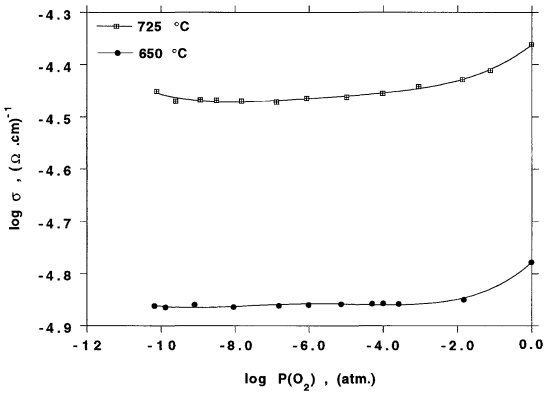

Fig. 1. Equilibrium Conductivity of undoped SBT as a function of $P_{(O_2)}$ for $T = 650°C$ and $T = 725°C$.

3. Results and Discussion

The crystal structure of SBT, which was originally considered to be face-centered-orthorhombic with space group *Fmmm* [8], has recently been refined to be A-centered-orthorhombic with space group $A2_1am$ [9]. This refined symmetry preserves the originally accepted two-layer structure of SBT, which is formed by the alternating fluorite-like $(Bi_2O_2)^{2+}$ and the perovskite-like $(SrTa_2O_7)^{2-}$ layers. We have confirmed the structure of our calcined undoped SBT powders by fully indexing the observed peaks of the XRD spectrum according to $A2_1am$ symmetry.

The results of the 4-probe dc high temperature equilibrium conductivity measurements that were performed on undoped SBT samples can be seen in Fig. 1.

The conductivity curves generally have slight upturns at the extreme ends of the oxygen activity range and a centrally located broad plateau. This is reminescent of the $P_{(O_2)}$ independent conductivity behavior of an oxygen vacancy concentration compensating a net acceptor excess as in ZrO_2 and CeO_2 doped with CaO [10].

The measurements were not carried out below about 10^{-10} atm., because electrical noise abruptly increased above its already high value.

Ionic transport number measurements were used to determine any possible transition in the identity of the charge carriers making the largest contribution to conductivity as the oxygen activity is reduced from that of pure oxygen. The results of the approximate ionic transport number measurements in Fig. 2 demonstrate that the ionic contribution to the total conductivity is large and increases as $P_{(O_2)}$ is reduced to the region where the conductivity becomes independent of oxygen activity.

The identity of the charge carriers making the largest contribution to total conductivity in the high oxygen activity region, where a prominent upturn occurs, is of interest. Thermopower measurements were made, using a heat pulse technique, in order to determine the identity of the charge carriers in pure oxygen, assuming they are electronic. Figure 3 represents the emf developed across the SBT sample as a function of the voltage signal proportional to the temperature gradient imposed. The positive sense of the slope of the curve demonstrates that the electronic

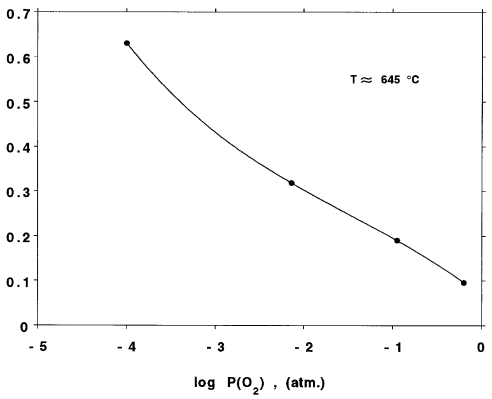

Fig. 2. The ionic transport number of undoped SBT as a function of the logarithm of the arithmetic average of the values of the oxygen activities that exist on each side of the sample at about 645°C.

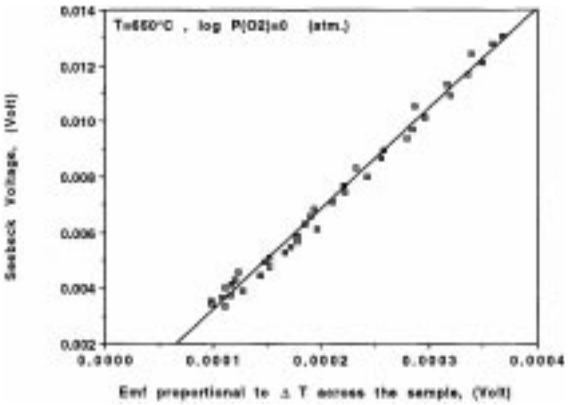

Fig. 3. The Seebeck voltage as a function of ΔT across the two ends of an undoped SBT sample for $T = 650°C$ and $\log P_{(O_2)} = 0$ (atm.). The positive slope indicates p-type conductivity.

carriers are holes. This is to be expected for an acceptor-doped oxide, for as the oxygen vacancies are partially filled in an oxidizing ambient, each of the incoming oxygen atoms captures two electrons from the lattice, creating two holes.

The results are consistent with the behavior of a material with a net acceptor excess whose equilibrium defect diagram is reproduced in Fig. 4 for a generic oxide MO [10]. The conductivity plateaus in Fig. 1 can be attributed to the horizontal line that represents the oxygen vacancy concentration $V_O^{\bullet\bullet}$ compensating a constant concentration of net acceptor excess $[A']$ which can be described by the approximate charge neutrality expression

$$[A'] \approx 2[V_O^{\bullet\bullet}] \tag{1}$$

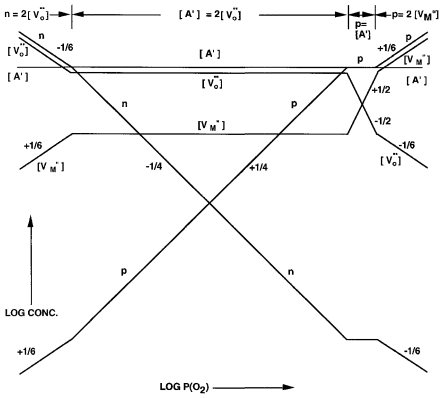

Fig. 4. Equilibrium defect diagram for an acceptor-doped metal oxide, assuming no electron or hole traps (adapted from [10]).

Further evidence to support the hypothesis that undoped SBT displays acceptor excess behavior, and an approximate quantitative estimate of the acceptor concentration can be obtained by performing 4-point dc conductivity measurements on acceptor-doped (Ti'_{Ta}) and donor-doped ($La^{\bullet}_{Sr}$) SBT. It can be seen in Fig. 5 that at dopant levels of 1%, the curves have the general qualitative features which are consistent with Fig. 4.

The upturns at the high and low $P_{(O_2)}$ ends of the curves in Fig. 5 can be related to the increasing concentration of holes $h^{\bullet}$ with a log-log slope $+\frac{1}{4}$ as a result of partial filling of oxygen vacancies $V_O^{\bullet\bullet}$, and electrons e' with a log-log slope $-\frac{1}{4}$ due to reduction of the lattice, respectively. This behavior is illustrated in Fig. 4.

In order to understand the dependence of electron and hole concentrations on $P_{(O_2)}$ and temperature, one has to first consider the oxidation reaction where an oxygen vacancy is filled by an incoming oxygen atom which creates two holes by capturing two electrons from the lattice. This corresponds to the reaction

$$\frac{1}{2}O_2 + V_O^{\bullet\bullet} \leftrightarrow O_O + 2h^{\bullet} \tag{2}$$

whose mass action expression is written as

$$\frac{p^2[O_O]}{[V_O^{\bullet\bullet}]P_{(O_2)}{}^{1/2}} = K_{ox}\exp(-\Delta H_{ox}/kT) \tag{3}$$

where k, T, p, O_O, K_{ox}, and ΔH_{ox} represent Boltzmann's constant, temperature, the hole concentration in the valence band, an oxygen ion located at

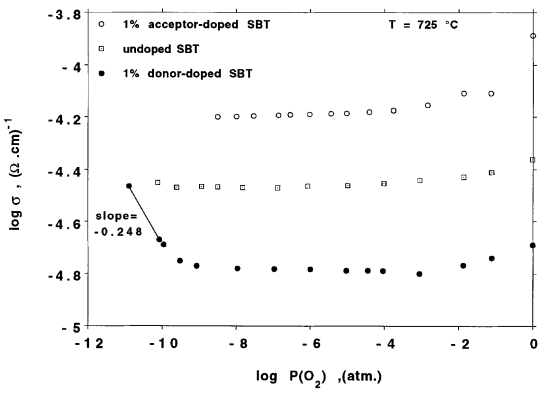

Fig. 5. The equilibrium conductivities of 1% acceptor-doped (Ti'_{Ta}), undoped, and 1% donor-doped ($Bi^{\bullet}_{Sr}$) SBT at 725°C.

its regular site in the lattice, the pre-exponential multiplier, and the enthalpy of oxidation, respectively.

Equations (1) and (3) can be combined in order to solve for p which is given as

$$p = \left\{\frac{K_{ox}[A']}{2[O_O]}\right\}^{1/2} P_{(O_2)}^{1/4} \exp(-\Delta H_{ox}/2kT) \tag{4}$$

which produces the log-log dependence of p on $P_{(O_2)}$ with the slope of $+\frac{1}{4}$. The intrinsic ionization process, in which electrons from the valence band are excited into the conduction band, may be expressed by the familiar expression

$$nil \leftrightarrow e' + h^{\bullet} \tag{5}$$

whose associated mass action expression is written as

$$np = K_i \exp(-E_g/kT) \tag{6}$$

where n, K_i, and E_g are the electron concentration in the conduction band, pre-exponential multiplier and the band gap, respectively. Combining Eqs. (4) and (6) in order to solve for n gives

$$n = \left\{\frac{2\ K_i^2\ [O_O]}{K_{ox}\ [A']}\right\}^{1/2} P_{(O_2)}^{1/4}$$

$$\exp\left\{\frac{-(E_g - \Delta H_{ox}/2)}{kT}\right\} \tag{7}$$

The significant emergence of electrons in Fig. 5 with log-log dependence of n on $P_{(O_2)}$ with the approximate slope $-\frac{1}{4}$ in 1% donor-doped ($La_{Sr}^{\bullet}$) SBT can be explained by the linear decrease of $[V_O^{\bullet\bullet}]$ with decreasing net acceptor excess $[A']$ and the increase of n with the relation $n \propto [A']^{-1/2}$ as given by Eqs. (1) and (7), respectively.

The conductivity of oxygen vacancies can be generally represented by $2e\ [V_O^{\bullet\bullet}]\mu(T)$, where e is the electronic charge and $\mu(T)$, the mobility of oxygen vacancies, is assumed to be only a function of temperature T. The conductivity corresponding to the plateau of undoped SBT can be expressed as $e[A']\mu(T)$ where the approximate charge neutrality expression $2[V_O^{\bullet\bullet}] \approx [A']$ is utilized. Ionic mobility can be given by the expression, $\mu^o/T\ \exp(-H_m/kT)$, where H_m and μ^o are the activation energy of ionic mobility and mobility pre-exponential multiplier, respectively. Then the ionic conductivity $\sigma_{V_O^{\bullet\bullet}}$ due to a constant concentration of oxygen vacancies compensating a net acceptor excess can be given as

$$\sigma_{V_O^{\bullet\bullet}} = \frac{\mu^o e[A']}{T}\ \exp(-H_m/kT) \tag{8}$$

Results of further 4-point dc conductivity measurements made only in the $P_{(O_2)}$ independent plateau at various temperatures in order to determine the thermal dependence of conductivity can be seen in Fig. 6. An Arrhenius plot of $T\sigma_{V_O^{\bullet\bullet}}$ for $\log P_{(O_2)} = -6.8$ (atm.) is seen in Fig. 7. The activation energy of motion is obtained as 0.94 eV which is a typical value for oxygen vacancies in perovskites and in the general range for other metal oxides.

SBT with an added donor content of 1% retains the apparent acceptor-doped behavior of undoped SBT, although at a reduced level. An approximate magnitude of the net acceptor excess in undoped SBT can be estimated by comparing the conductivity values corresponding to the plateaus in Fig. 5.

If it is assumed that the net acceptor dopant concentration in 1% acceptor-doped SBT and 1% donor-doped SBT can be given as $[A'] + 0.01$ and $[A'] - 0.01$, respectively, then the isothermal conductivities of acceptor-doped, undoped and donor-doped SBT in the plateau region can be related to each other as: $\sigma_A : \sigma_U : \sigma_D = ([A'] + 0.01) : ([A']) : ([A'] - 0.01)$. σ_A, σ_U and σ_D are the conductivities of acceptor-doped, undoped and donor-doped SBT, respectively.

Using the conductivity values from Fig. 5, one determines $[A']$ as being between 1% and 2%. Acceptor doping due to unintentional presence of

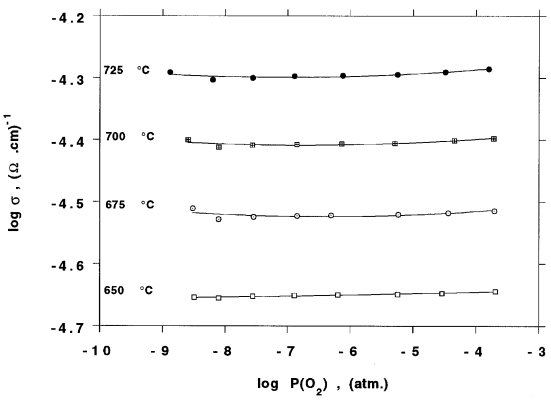

Fig. 6. The equilibrium conductivity of undoped SBT at lower oxygen activities for values of temperature at 25°C intervals between 650°C and 725°C.

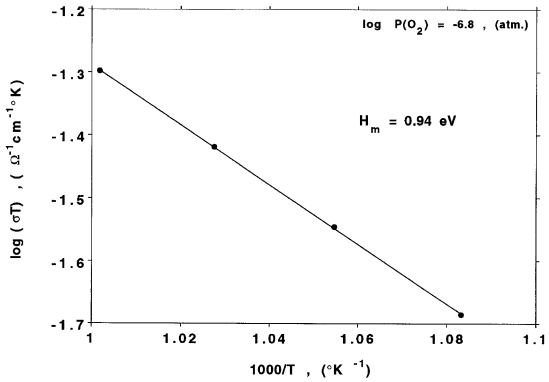

Fig. 7. An Arrhenius plot of of log(σT) for undoped SBT at log $P_{(O_2)} = -6.8$ (atm.).

impurities is common, but at levels two orders of magnitude lower [17,18].

The large value of the concentration of acceptor centers ($[A'] \approx 1 - 2\%$) found in undoped SBT needs to be justified. The magnitude of the concentration, the purity of starting powders (given in Table 1), and the reproducibility of experiments with samples processed from different batches of calcined powders suggest that processing-related accidental presence of impurities is not the source of the acceptor centers. On the other hand, detailed structural studies of layered bismuth oxides recently made by [9] and [19] have indicated that there is significant place exchange, several percent, between the Sr^{2+} and Bi^{3+} ions, creating donor centers $Bi_{Sr}^{\bullet}$ in the perovskite-like layers and acceptor centers Sr'_{Bi} in the bismuth oxide layers. In a different material with a homogeneous unit cell that does not have a layered structure, such place exchange should be completely self-compensating and not require the presence of any other compensating defects. On the other hand, it is important to note that our experimental findings presented thus far in this paper have created a dilemma which can be defined as the combination of three independent observations:

1. SBT has an intrinsic superior ferroelectric fatigue endurance [20];
2. High oxygen vacancy concentrations have been linked to poor fatigue performance in perovskite ferroelectrics [2–5];
3. Our defect chemistry results indicate that there is a very large concentration, about 1%, of oxygen vacancies in SBT.

In order to elucidate this dilemma, we postulate that each layer of the structure of SBT acts as a distinct sub-system with its own defect chemistry. Thus for the bismuth oxide layers, the acceptor centers Sr'_{Bi} created by the cation place exchange are partially compensated by positively-charged defects within those layers, e.g., $[V_O^{\bullet\bullet}]$. Similarly for the perovskite-like layers, the donor centers $Bi_{Sr}^{\bullet}$ created by the place exchange are partially compensated by negatively-charged defects within those layers. Some part of the Sr'_{Bi} and $Bi_{Sr}^{\bullet}$ concentrations may be self-compensating across the boundaries of the two adjacent layers. The ferroelectric response of SBT is localized in the perovskite-like layers [9,16,19]. One can then postulate that the observed ionic conductivity is due to oxygen vacancies confined within the acceptor-doped bismuth oxide layers, where they cannot interfere with the ferroelectric response of the perovskite-like layers. Because the perovskite-like layers are effectively donor-doped, the oxygen vacancy concentration within those layers will be strongly suppressed. It is the separation of the structure of SBT into two parallel sub-systems that allows the presence of a high concentration of oxygen vacancies in a material that shows exceptional resistance to ferroelectric fatigue.

It is of interest to depict the cation place exchange, which occurs while the compound is being processed, with incorporation reactions. A comparison of the equilibrium conductivity experiments performed on SBT (Fig. 1) and SBN [12] with the Kröger-Vink diagrams of acceptor-doped oxides and donor-doped oxides [10], respectively, indicate that the Sr'_{Bi} and $Bi_{Sr}^{\bullet}$ centers should be compensated by ionic defects at high oxygen activities (the SBT and SBN samples are processed in air). Therefore, the incorporation reactions that produce compensating ionic point defects are preferred. The cation place exchange process can be described by two alternative sets of incorporation reactions that create compensating ionic point defects. One set would involve the exchange of two units of SrO with one unit of Bi_2O_3 between the adjacent layers and would ideally fill the cation sites vacated by the units involved ($2SrO \leftrightarrow Bi_2O_3$):

$$Bi_2O_3 \xrightarrow{(2SrO)} 2Bi_{Sr}^{\bullet} + 2O_O + O_I'' \qquad (9)$$

$$2SrO \xrightarrow{(Bi_2O_3)} 2Sr'_{Bi} + 2O_O + V_O^{\bullet\bullet} \qquad (10)$$

The other alternative set of reactions involves an

exchange of three units of SrO with one unit of Bi_2O_3 which would ideally fill the anion sites vacated by the units involved ($3SrO \leftrightarrow Bi_2O_3$):

$$Bi_2O_3 \xrightarrow{(3SrO)} 2Bi_{Sr}^{\bullet} + 3O_O + V_{Sr}'' \qquad (11)$$

$$3SrO \xrightarrow{(Bi_2O_3)} 2Sr_{Bi}' + 3O_O + Sr_I^{\bullet\bullet} \qquad (12)$$

$$3SrO + Bi_{Bi} + 3/2O_O \xrightarrow{(Bi_2O_3)} 3Sr_{Bi}' + 3O_O + 3/2V_O^{\bullet\bullet} + 1/2Bi_2O_3 \qquad (13)$$

The oxygen interstitial O_I'' is not a favorable defect in the perovskite layers, therefore, the first set of reactions represented by Eqs. (9) and (10) are considered to be unlikely. On the other hand, the reactions represented by Eqs. (12) and (13) are two possible ways of incorporating 3 units of SrO into the bismuth oxide layers. Equation (12) is an unlikely reaction because $Sr_I^{\bullet\bullet}$ is not a favorable defect. This leaves us with Eqs. (11) and (13) in the second set of reactions which involve the favorable ionic vacancies V_{Sr}'' and $V_O^{\bullet\bullet}$. Moreover, Eq. (13) suggests the formation of a Bi_2O_3 phase which will be discussed shortly. Equation (11) justifies the approximate charge neutrality expression that is valid in the perovskite-like layers for the high oxygen activity region in which SBT is processed:

$$[Bi_{Sr}^{\bullet}] \approx 2[V_{Sr}''] \qquad (14)$$

Equation (13), whose corresponding approximate charge neutrality expression can be written as

$$[Sr_{Bi}'] \approx 2[V_O^{\bullet\bullet}] \qquad (15)$$

is valid in the bismuth oxide layers. The cation place exchange described by Eqs. (11) and (13) can be depicted by the cartoon in Fig. 8. The six disordered Sr ions, Sr_{Bi}', are locally compensated by three oxygen vacancies $V_O^{\bullet\bullet}$ in the bismuth oxide layer. On the other hand, four of the six displaced Bi ions $Bi_{Sr}^{\bullet}$ are locally compensated by two Sr vacancies V_{Sr}'' in the perovskite-like layer. As indicated by Eq. (13), the other two Bi and three O atoms can only be accommodated on the surfaces or grain boundaries in order to form Bi_2O_3.

A strong evidence for a bismuth-rich phase deposited on the surfaces has recently been provided by Ono et al. [21] who used glow discharge optical emission spectrometry (GDS) in order to obtain elemental depth profiles. The results indicated that the Bi concentration was higher at the surface than in the interior of the solution-deposited SBT films, whereas Sr and Ta concentrations were found to be uniform.

In addition, we see scattered, yellow-colored stains on the surface of our sintered SBT. They have a glassy appearance as if they had been melted. Qualitative Energy-Dispersive Spectroscopy (EDS) measurements indicate that these stains are slightly bismuth-rich relative to other areas of the surface.

The results of band structural studies performed by [14] and spectroscopic studies by [13], although not in good agreement with each other, indicate that SBT has a relatively large band gap. Diffraction studies by [19] have revealed that place exchange occurs between Bi^{3+} and Sr^{2+} in the alternating layers. It is suggested by Eqs. (13) and (15) that $[Sr_{Bi}']$ is partially compensated by oxygen vacancies in the fluorite-like bismuth oxide layers. We can then substitute $[Sr_{Bi}']$ for $[A']$ in Eq. (1). Consequently, the conductivity

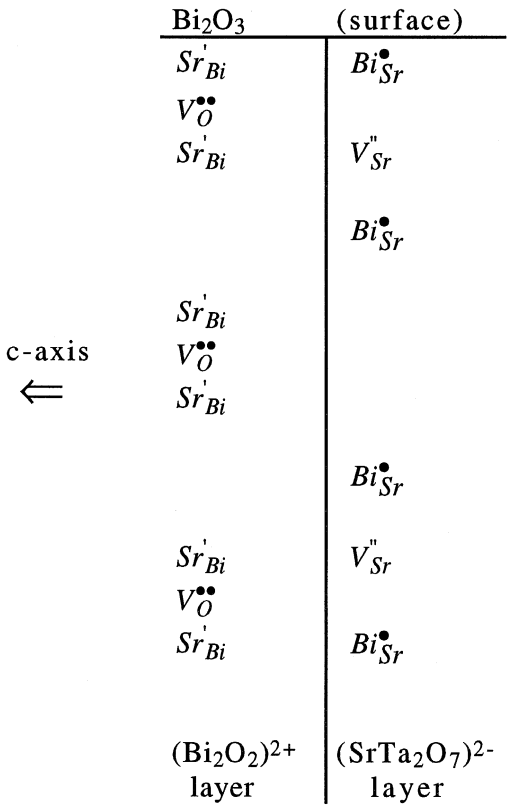

Fig. 8. A cartoon which depicts local charge compensation of cation place exchange by defect formations in the two different layers of the crystal structure of SBT and consequent deposition of Bi_2O_3 at surfaces.

behavior of SBT can be attributed to p-type conductivity at high oxygen activities and oxygen vacancy transport at lower values of $P_{(O_2)}$, both of which occur in the bismuth oxide layers that have a net 1–2% acceptor excess, $[Sr'_{Bi}]$, and a large band gap. On the other hand, Eqs. (11) and (14) suggest that the $[Bi^{\bullet}_{Sr}]$ concentration, which is partially compensated at high oxygen activities by $2[V''_{Sr}]$, creates a net donor excess in the perovskite-like layers. Strontium vacancies, which are practically immobile, would be replaced by an electron concentration created as a result of the reduction reaction at lower oxygen activities, but the mobility of electrons in the perovskite-like layers of SBT is also very low [12]. Therefore, the total conductivity of SBT is dominated by oxygen vacancies, transported in the bismuth oxide layers, whose energetic cost of conductivity, as expressed by Eq. (8), is merely due to the energy of activation of mobility (0.94 eV).

It was reported by Ono et al. [11,21] that XPS studies revealed the existence of metallic bismuth on the surface of solution-deposited SBT thin films. It can be seen in Fig. 9a that our own XPS studies performed on the surface of bulk SBT confirm the existence of metallic bismuth. It can be seen in Fig. 9b that XPS measurements made on a fresh fracture surface of a sintered SBT specimen broken in the ultra-high vacuum chamber, display no evidence of metallic bismuth. The extremely reducing conditions comprised by the combined effects of ultra-high vacuum and high-energy particle/photon beams that a sample is exposed to in SEM/TEM/XPS experiments appear to be creating the metallic bismuth that is observed on the surface of stoichiometric samples. The difference between the spectra in Figs. 9a and 9b may be explained by the longer period of time that the sample surface is exposed to the ultra-high vacuum and Al Kα radiation than the shorter duration that a freshly prepared fracture surface spends under those conditions.

This justification of metallic bismuth presence is supported by the results of our XPS measurements (to be presented in a different publication) performed on the freshly-prepared fracture surface of an undoped $SrBi_2Nb_2O_9$ sample, where a strong signal emanating from metallic bismuth core levels (4f states) was obtained from the fracture surface after it was exposed overnight to the ultra-high vacuum, Al Kα, and 5 eV electron flood gun in the XPS system, even though initial XPS measurements on the same fracture surface, prior to this exposure to the extremely reducing conditions, displayed no metallic bismuth presence.

Furthermore, based on the local charge compensation model proposed above, the p-type conductivity observed at high oxygen activities in Fig. 1 and the Kröger-Vink model shown in Fig. 4 suggest that the bismuth oxide layers are exposed to an oxidizing atmosphere while they are being calcined/sintered in air; therefore, formation of metallic bismuth from a starting powder of Bi_2O_3 in the initial mixture is not likely. The particular processing conditions that exist during the alkoxide-based solution deposition of SBT thin films may be enhancing the formation of metallic bismuth observed by [11,21]. The concentration gradient of hydrogen which indicates a significantly larger presence at the surface of the SBT films,

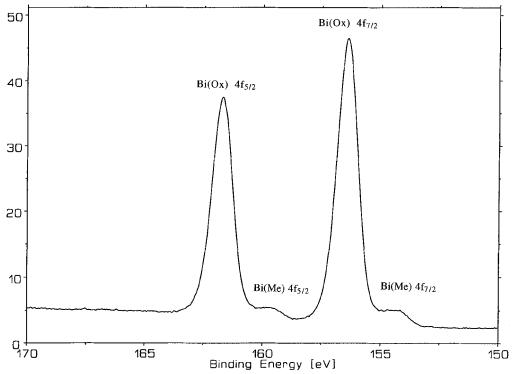

Fig. 9a. Core level XPS signal from Bi^{3+} 4f(ox) and metallic Bi 4f(me) states on the surface of SBT.

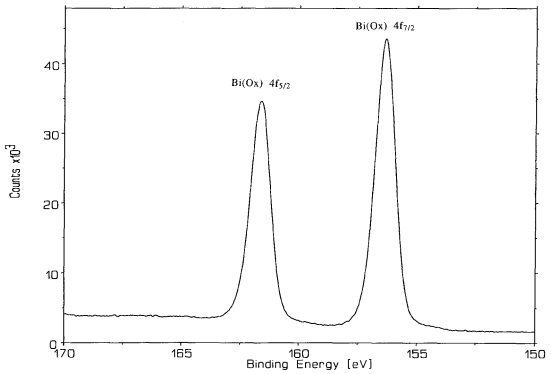

Fig. 9b. Core level XPS signal from Bi^{3+} 4f(ox) on a freshly-formed fracture-surface of SBT.

paralleling the concentration profile of bismuth, suggests that hydrogen could be playing a role as a reducing agent in the formation of metallic bismuth from the Bi_2O_3 deposited on the surfaces or grain boundaries.

4. Conclusions

1a. The equilibrium electrical conductivity of SBT is dominated by ionic defects (presumably oxygen vacancies) at low oxygen activities and holes at high oxygen activities.

1b. This conductivity behavior for undoped SBT is consistent with that of an oxide that has 1–2% net acceptor excess, compensated by oxygen vacancies, and low electronic conductivity.

2a. We postulate that the observed conductivity behavior is restricted to the bismuth oxide layers, where there is a large net acceptor excess which is attributed to the Sr'_{Bi} centers that are formed as a result of place exchange between Sr^{2+} and Bi^{3+} ions.

2b. We postulate that the Sr'_{Bi} centers are locally compensated in the bismuth oxide layers which act as distinct sub-systems whose defect chemistry behavior is typical of an acceptor-doped metal oxide.

3. Similarly, we postulate that the perovskite-like layers, which have a large net donor excess due to the $Bi^{\bullet}_{Sr}$ centers created by the cation place exchange process, act as distinct sub-systems whose defect chemistry behavior is typical of a donor-doped metal oxide.

4. The concentration and mobility of electrons are expected to be low in the perovskite-like layers. Thus the total conductivity of SBT is dominated by the better conducting layers which are the bismuth oxide layers.

5. The explanation for the superior intrinsic ferroelectric fatigue endurance of SBT can be constructed in the following steps:
   (i) In perovskite compounds electronic charge trapped at the ferroelectric domain boundaries pin the domain walls and suppress the switchable polarization of the domains. The trapped charge can become stabilized if there are oxygen vacancies nearby.
   (ii) Perovskite layers of SBT create the ferroelectric response [9,16,19].
   (iii) The electron mobility in the perovskite-like layers of SBT is very low. Electrons do not easily drift under applied electric fields and thus do not accumulate at the domain boundaries.
   (iv) Oxygen vacancies, which do not enter the perovskite-like layers containing a large concentration of donor centers $Bi^{\bullet}_{Sr}$, are mostly confined to the bismuth oxide layers. If an oxygen vacancy moved from the bismuth oxide layer to the perovskite-like layer, accompanying new defects would have to be created in order to balance the change in each layer; this would have an enthalpic cost.
   (v) The large concentration 1–2% of donor centers $Bi^{\bullet}_{Sr}$ in the perovskite-like layers of SBT suppress the influence of any naturally occurring acceptor impurities which otherwise could be compensated by detrimental oxygen vacancies in the perovskite-like layers.
   (vi) Therefore, the perovskite-like layers, which create the ferroelectric response of SBT, are free of mobile defects that would otherwise accumulate under applied electric fields at the domain walls and interfere with their motion.

6. It is suggested that the observation of the presence of metallic bismuth in the XPS measurements is an experimental artifact created by the extremely reducing conditions that exist in the XPS system.

Acknowledgment

The authors are grateful for financial support by the Division of Materials Research of the National Science Foundation.

The authors of this research (project) acknowledge the allocation of time and services in the SCIENTA ESCA laboratory of Lehigh University. Professional and technical assistance (guidance) of Dr. Alfred C. Miller is greatly appreciated.

References

1. O. Auciello, J.F. Scott, and R. Ramesh, *Physics Today*, **51**(7), 22 (1998).
2. W.L. Warren, D. Dimos, B.A. Tuttle, and D.M. Smyth, *J. Am. Ceram. Soc.*, **77**, 2753 (1994).

3. R. Waser, T. Baiatu, and K.-H. Härdtl, *J. Am. Ceram. Soc*., **73**, 1645 (1990).
4. H.M. Duiker, P.D. Beale, J.F. Scott, C.A. Paz de Araujo, B.M. Melnick, J.D. Cuchiaro, and L.D. Millan, *J. Appl. Phys*., **68**, 5783 (1990).
5. W.L. Warren, B.A. Tuttle, and D. Dimos, *App. Phys. Lett*., **67**(10), 1426 (1995).
6. E.C. Subbarao, *J. Am. Ceram. Soc*., **45**, 166 (1962).
7. P.C. Eklund and A.K. Mabatah, *Ref. Sci. Instrum*., **48**, 775 (1977).
8. B. Aurivillius, *Arki. Kemi*., **1**, 463 (1949).
9. A.D. Rae, J.G. Thompson, and R.L. Withers, *Acta Crystallogr., Sect. B*., **48**, 418 (1992).
10. D.M. Smyth, *Prog. Solid State Chem*., **15**, 145 (1984).
11. S. Ono, A. Sakakibara, T. Seki, T. Osaka, I. Koiwa, J. Mita, T. Iwabuchi, and K. Asami, *J. Electrochem. Soc*., **144**, L185 (1997).
12. A.C. Palanduz and D.M. Smyth, *J. Euro. Ceram. Soc*., **19**, 731 (1998).
13. A.J. Hartmann, R.N. Lamb, J.F. Scott, and C.D. Gutleben, *Integrated Ferroelectrics*., **18**, 101 (1997).
14. J. Robertson, C.W. Chen, W.L. Warren, and C.D. Gutleben, *Appl. Phys. Lett*., **69**, 1704 (1996).
15. H.N. Al-Shareef, D. Dimos, T.J. Boyle, W.L. Warren, and B.A. Tuttle, *Appl. Phys. Lett*., **68**(5), 690 (1996).
16. R.L. Withers, J.G. Thompson, and A.D. Rae, *J. Solid State Chem*., **94**, 404 (1991).
17. N.H. Chan, R.K. Sharma, and D.M. Smyth, *J. Am. Ceram. Soc*., **65**, 167 (1982).
18. N.H. Chan and D.M. Smyth, *J. Am. Ceram. Soc*., **67**, 285 (1984).
19. S.M. Blake, M.J. Falconer, M. McCreedy, and Philip Lightfoot, *J. Mater. Chem*., **7**(8), 1609 (1997).
20. C.A. Paz de Araujo, J.D. Cuchlaro, L.D. McMillan, M.C. Scott, and J.F. Scott, *Nature (London)*, **374**, 627 (1995).
21. S. Ono, A. Sakakibara, T. Osaka, I. Koiwa, J. Mita, and K. Asami, *J. Electrochemi. Soc*., **146**(2), 685 (1999).